

A Quantitative Model of Human Jejunal Smooth Muscle Cell Electrophysiology

Weiwei Ai^{1*} and David P Nickerson¹

¹Auckland Bioengineering Institute, University of Auckland, New Zealand

ORIGINAL

Abstract

The Poh et al. (2012) paper describes the first biophysically based computational model of human jejunal smooth muscle cell (hJSMC) electrophysiology. The ionic currents are described by either a traditional Hodgkin-Huxley (HH) formalism or a deterministic multi-state Markov (MM) formalism. We create a modularized CellML implementation of the model, which is able to reproduce clamping behaviours of individual currents and whole cell action potential traces. In addition, some inconsistencies have been uncovered and discussed in this paper.

Keywords: Human jejunal smooth muscle cell, computational model, CellML

Curated Model Implementation

<http://doi.org/10.36903/physiome.16590317>

Primary Publications

Y. C. Poh, A. Corrias, N. Cheng, and M. L. Buist. A quantitative model of human jejunal smooth muscle cell electrophysiology. 2012.

OPEN ACCESS Reproducible Model

Edited by
Shelley Fong

Curated by
Anand Rampadarath

**Corresponding author*
weiwei.ai@auckland.ac.nz

Submitted 09 Aug 2021

Accepted 09 Sept 2021

Citation
Ai and Nickerson
A Quantitative Model of
Human Jejunal Smooth
Muscle Cell
Electrophysiology. *Physiome*.
doi: 10.36903/physiome.16590317

1 Introduction

In the primary paper (Poh et al., 2012), the first biophysically based model of human jejunal smooth muscle cell (hJSMC) electrophysiology was presented. Here, we divide the mathematical model into distinct sub-modules encoded in CellML enabling reuse of the various sub-modules in future studies and models. We attempt to reproduce individual ionic currents, cellular voltage behaviour and sensitive analysis corresponding to changes of channel conductance. From the primary paper we extracted data using the Engauge digitizer software (Mitchell et al., 2020) to compare the current simulation results against those in the primary publication. In doing so, we found inconsistencies in parameter values and mathematical equations presented in the primary paper, as well as the simulation experiment settings. These discrepancies are discussed in [section 4](#).

2 Model description

2.1 Primary Publication

In the hJSMC model (Poh et al., 2012), L-type calcium channels, the large conductance calcium and voltage activated potassium channels (BK) channels, and sodium channels are formulated using a deterministic multi-state Markov (MM) model (Sakmann and Neher, 1996), while the T-type calcium channels and voltage dependent potassium current employ a traditional Hodgkin-Huxley (HH) formalism (Hodgkin and Huxley, 1952). The sodium calcium exchanger and sodium potassium pump formulation are based on the work proposed by ten Tusscher et al. (2004). The primary publication shows that the model has been validated against a wide range of experiments and data. The authors also provide CellML code https://models.physiomeproject.org/w/yc_poh/poh_

2012 and C code https://computationalbiolab.github.io/jejunal_smc_model/. The mathematical descriptions in the publication (Poh et al., 2012) along with these codes are the basis to build the curated CellML implementation presented here.

2.2 Modularized CellML model

The modularized version of the CellML implementation is available on Physiome Model Repository (PMR) at <https://models.physiomeproject.org/workspace/692> and the documentation can be found in the corresponding exposure at <https://models.physiomeproject.org/e/6c7>. In this manuscript we focus on reproducibility and reusability. The main components of this model and the performed simulation experiments are summarized as follows.

The *membrane potential component* defines the complete equations of the membrane potential and total ionic current. It combines the imported ionic current components and ionic concentrations components. The component can be stimulated by various periodic stimuli and generates a sequence of action potentials. The *clamped current component* defines the complete equations of the total and individual ionic currents, when performing voltage or concentration clamp simulation experiments.

The individual *ionic current components* share the same formulation $I = g_{max} PO(V_m - E)$, where V_m is the membrane potential and $E = \frac{RT}{zF} \ln\left(\frac{X_o}{X_i}\right)$ is the reversal potential defined in the *Nernst potential component*. The open probability PO computation depends on the formalism. For L-type calcium channels, the large conductance calcium and voltage activated potassium channels (BK) channels, sodium channels, a deterministic multi-state Markov (MM) model (Sakmann and Neher, 1996) is used to describe various channel states. Such currents incorporate the *channel states* components. The Hodgkin-Huxley (HH) formalism of the T-type calcium channels and voltage dependent potassium current includes the *gating kinetics* components along with steady state of gates and time constants components. The sodium calcium exchanger and sodium potassium pump formulation is different from the aforementioned currents, which is defined in its own component.

The *ionic concentrations component* defines the dependence of the intracellular concentrations on the membrane currents. The *temperature factor component* encodes the temperature coefficient $\phi = Q_{10}^{\frac{T-T_0}{10}}$, where Q_{10} is species specific parameter, T_0 is the reference temperature (i.e., the model construction temperature), and T is the desired temperature for a given simulation experiment. This coefficient is included in the equations listed in Table 3.

Following best practices, our CellML implementation separates the mathematics from the parameterisation of the model. The mathematical model is imported into a specific parameterised instance in order to perform numerical simulations. The parameterisation would include defining the stimulus protocol to be applied. We have three sets of simulation experiments and corresponding simulation results to reproduce the corresponding figures in the primary publication:

1. the *patch clamp experiment* is used to validate the individual ionic currents;
2. the *periodic stimulation experiment* is used to generate a sequence of action potentials; and
3. the *sensitivity analysis experiment* is used to evaluate the contributions of currents to the membrane voltage.

Simulation settings and detailed solver information are encoded in SED-ML documents for execution of the simulation experiments (Waltemath et al., 2011). The Python scripts used with OpenCOR (Garny and Hunter, 2015) to perform simulations and produce the figures in the primary paper are also included in the folder <Simulation>. The name of the simulation and plot scripts indicate the figure number in the primary paper. For example, Fig2_sim.py is used to generate the simulation data and Fig2_plot.py reproduces the graph shown in Figure 2 from Poh et al. (2012).

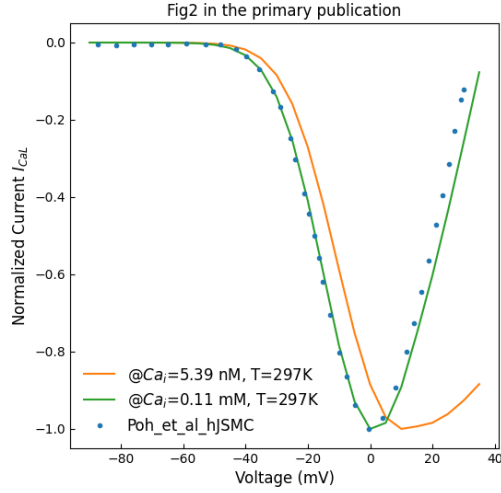


Figure 1. Normalized L-type Ca^{2+} channels peak I-V plot (c.f., Fig. 2 in Poh et al. (2012)).

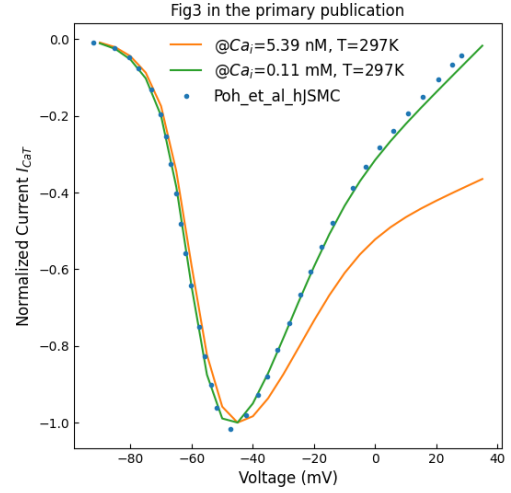


Figure 2. Normalized T-type Ca^{2+} channels peak I-V plot (c.f., Fig. 3 in Poh et al. (2012)).

3 Model results

3.1 Response of individual ionic currents to clamped voltage

In the *patch clamp experiment*, the *clamped current component* is configured and parameterised with an applied *patch clamp protocol*. The clamping parameters can be changed by the user, while the values used in this article are listed in Table 1. The holding voltage duration is 1 second and the temperature is 297 Kelvin. The simulation experiment can be performed by loading the corresponding SED-ML document into OpenCOR and executing the simulation. By increasing the intracellular concentrations, we have reproduced the IV curves in Figures 1, 2 and 5, however, the specific experiment settings cannot be confirmed by the authors.

Table 1. Clamping parameters

Fig	Holding voltage (mV)	Test voltages (mV)	Current	X_i (mM)
2	-100	-90:5:40	I_{CaL}	$Ca_i^{2+} = 5.388e-5, Ca_i^{2+} = 0.11$
3	-100	-90:5:40	I_{CaT}	$Ca_i^{2+} = 5.388e-5, Ca_i^{2+} = 0.11$
4	-70	-70:5:-15	I_{KV}	$K_i^+ = 153.6$
5	-70	-70:10:70	I_{BK}	$K_i^+ = 153.6, Ca_i^{2+} = 0.001, Ca_i^{2+} = 0.0003$
6	-100	-90:5:30	I_{Na}	$Na_i^+ = 10.57, Na_i^+ = 50$

In the presented figures, the dots denote the simulated data extracted from the primary publication, while the solid lines are the simulation results produced by the current CellML implementation.

Figure 1 shows the normalized L-type Ca^{2+} channels peak I-V plot with different intracellular concentrations. During simulation, the θ and δ in Equations S-33 and S-34 are set to 0 to switch off the Ca_i^{2+} dependency. Figure 2 shows normalized T-type Ca^{2+} channels peak I-V plot.

Figure 3 shows normalized I-V plot of whole cell voltage-activated potassium currents. The holding voltage was not specified in the primary paper, and we assume here a value of -70 mV.

Figure 4 shows open probability of BK channel versus clamping voltage at various intracellular calcium concentrations.

Figure 5 shows normalized sodium channel peak I-V plot various intracellular Na^+ concentrations.

Figure 6 shows whole cell normalized I-V data from hJSMC model under near calcium-free conditions. The intracellular Na^+ concentration is set to 10.57 mM, while the value is unknown

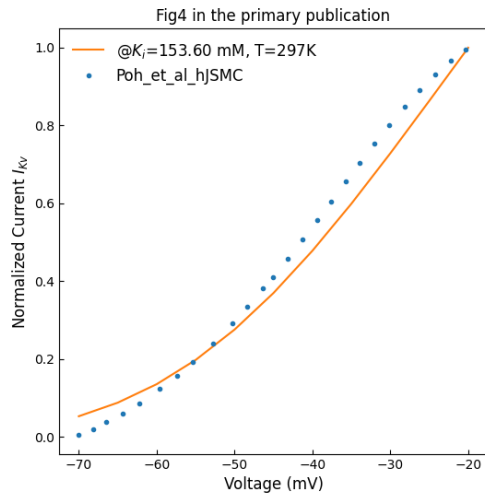


Figure 3. Normalized I-V plot of whole cell voltage-activated potassium currents (*c.f.*, Fig. 4 in Poh et al. (2012)).

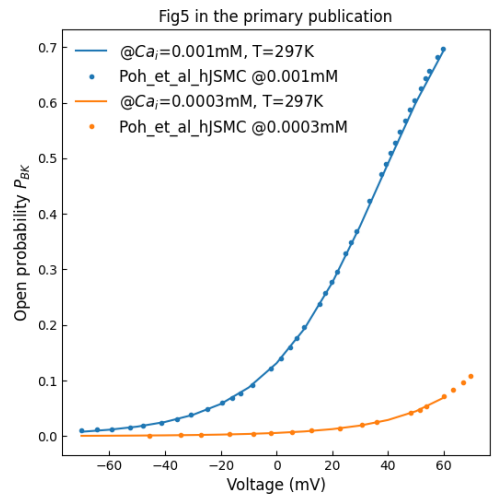


Figure 4. Open probability versus clamping voltage plots, across various free intracellular Ca^{2+} concentrations (*c.f.*, Fig. 5 in Poh et al. (2012)).

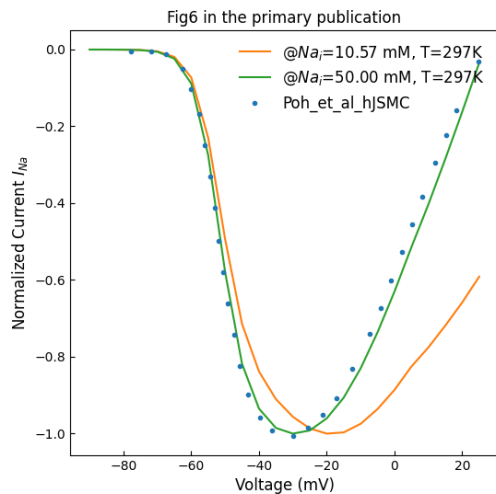


Figure 5. Normalized Na^+ channel peak I-V plot (*c.f.*, Fig. 6 in Poh et al. (2012)).

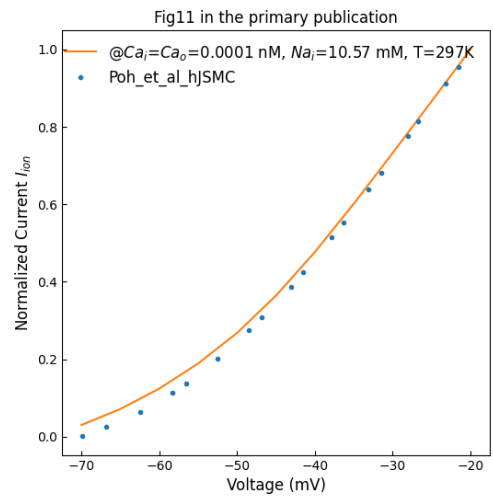


Figure 6. Simulated whole cell normalized I-V data under near calcium-free conditions (*c.f.*, Fig. 11 in Poh et al. (2012)).

in the primary publication.

3.2 Simulated action potentials

In the *periodic stimulation experiment*, the *membrane potential component* is configured and parameterised with a periodic stimulus current. The parameters of stimulation can be changed and the following simulation uses 310 Kelvin for the temperature setting.

Figure 7 shows the simulated hJSMC action potential trace and free intracellular calcium concentration after a simulation of 30 minutes of electrical activity.

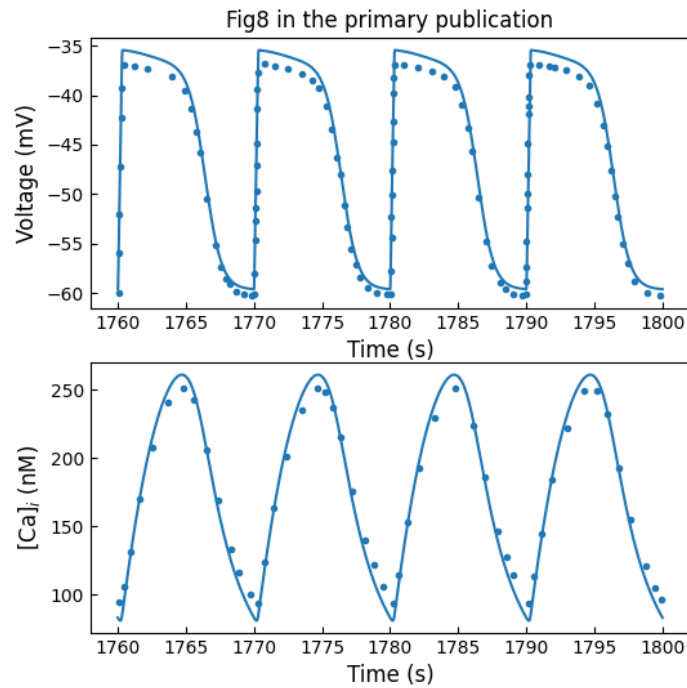


Figure 7. simulated hJSMC action potential trace and free intracellular calcium concentration after a simulation of 30 minutes of electrical activity (*cf.*, Fig. 8 in Poh et al. (2012)).

3.3 Sensitivity Analysis

In the *sensitivity analysis experiment*, the *membrane potential component* is configured to accept the changes of maximum conductance of ionic channels in the component $g_parameters$.

Figure 8 shows sensitivity analysis by 50% increase or decrease in maximum channel conductance. This evaluates the contributions of key ionic currents towards hJSMC membrane voltage. The last plot shows the free intracellular Ca^{2+} concentrations corresponding to changes in I_{CaL} .

4 Discussion

Based on the author provided model implementation (Poh et al., 2012), we modularized the CellML implementation for reusability. Additionally, we added clamped current component, patch clamp protocol and voltage clamp experiment to simulate ionic currents during a voltage clamp. We also modified the periodic current protocol and periodic stimulation experiment to enable the periodic stimulation for Figure 8.

During the curating process, we found some parameters (see Table 2) and equations (see Table 3) which are inconsistent from the ones presented in the primary publication.

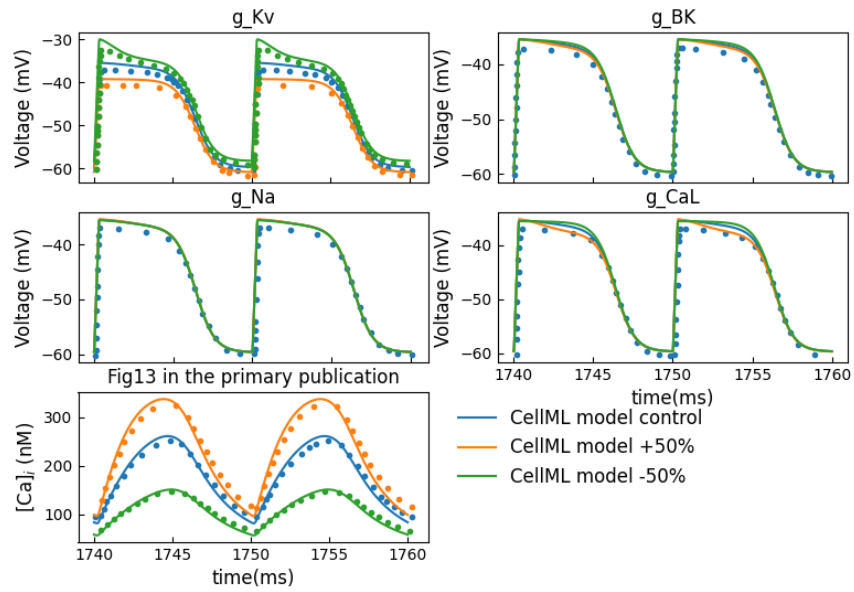


Figure 8. Sensitivity analysis by 50% increase or decrease in maximum channel conductance (c.f., Fig. 13 in Poh et al. (2012)).

Since the clamping values for intracellular concentrations of Ca_i^{2+} , Na_i^+ and K_i^+ were not specified in the paper, we used the initial values presented in the original CellML model in the first attempt. However, the difference becomes significant at less negative clamping voltages when reproducing the original Figures 2, 3, and 6. We then increased the intracellular concentrations for a better fit. However, the values of intracellular concentrations in particular Ca_i^{2+} are quite larger than physiological value, which should be aware of in future usage of this model.

Table 2. Inconsistency of parameters

Parameters	primary paper	Original CellML	C code	current CellML
P_{NCX}	39.8437	1992.335	1992.1865	1992.1865
P_{NaK}	0.1852	9.26	16.197	16.197
τ_{dCat}	1.9058	1.9058	1.9508	1.9508
1st factor in Eq(S-24)	0.05956	0.05956	0.005956	0.005956

Table 3. Inconsistency of equations

Equations	primary paper	Original CellML	C code	current CellML
S-5, S-6, S-7	without unit conversion	$\times 1e - 15$	V_{cell} in mm^3 and $\times 1e - 9$	$\times 1e - 15$
S-13, S-14	No T^1	with T^2	with T^2	with T^2 and $T_0 = 310K$
S-23, ..., S-28	No T^1	with T^2	with T^2	with T^2 and $T_0 = 310K$
S-33, S-34	No T^1	with T^2	with T^2	with T^2 and $T_0 = 310K$
S-36, S-37,	No T^1	with T^2	with T^2	with T^2 and $T_0 = 297K$
S-43, S-44	No T^1	with T^2	with T^2	with T^2 and $T_0 = 297K$
S-80, ..., S-91	No T^1	with T^2	with T^2	with T^2 and $T_0 = 297K$
S-67, ..., S-70	with Ca_i^{2+}	without Ca_i^{2+}	without Ca_i^{2+}	without Ca_i^{2+}
S-75, ..., S-78	with Ca_i^{2+}	without Ca_i^{2+}	without Ca_i^{2+}	without Ca_i^{2+}

¹ No temperature correction.

² Multiplied by corresponding temperature factor $\phi = Q_{10}^{\frac{T-T_0}{10}}$.

Acknowledgements

The authors gratefully acknowledge the assistance of Alberto Corrias and Martin Buist in the validation of the model implementation presented here.

References

- A. Garny and P. J. Hunter. OpenCOR: a modular and interoperable approach to computational biology. *Front Physiol*, 6, 2015. doi: 10.3389/fphys.2015.00026. URL <http://journal.frontiersin.org/article/10.3389/fphys.2015.00026/abstract>.
- A. L. Hodgkin and A. F. Huxley. A quantitative description of membrane current and its application to conduction and excitation in nerve. *The Journal of physiology*, 117(4):500–544, 1952.
- M. Mitchell, B. Muftakhidinov, T. Winchen, A. Wilms, B. v. Schaik, badshah400, Mo-Gul, T. G. Badger, Z. Jędrzejewski-Szmek, kensington, and kylesower. markummitchell/engage-digitizer: Nonrelease, July 2020. URL <https://doi.org/10.5281/zenodo.3941227>.
- Y. C. Poh, A. Corrias, N. Cheng, and M. L. Buist. A quantitative model of human jejunal smooth muscle cell electrophysiology. 2012.
- B. Sakmann and E. Neher. Single-channel recording. *General Pharmacology: The Vascular System*, 27(6):1078, 1996. ISSN 0306-3623. doi: [https://doi.org/10.1016/0306-3623\(96\)90073-7](https://doi.org/10.1016/0306-3623(96)90073-7). URL <https://www.sciencedirect.com/science/article/pii/0306362396900737>.
- K. H. ten Tusscher, D. Noble, P.-J. Noble, and A. V. Panfilov. A model for human ventricular tissue. *American Journal of Physiology-Heart and Circulatory Physiology*, 286(4):H1573–H1589, 2004.
- D. Waltemath, R. Adams, F. T. Bergmann, M. Hucka, F. Kolpakov, A. K. Miller, I. I. Moraru, D. Nickerson, S. Sahle, J. L. Snoep, and N. L. Novère. Reproducible computational biology experiments with SED-ML - The Simulation Experiment Description Markup Language. *BMC Systems Biology*, 5(1):198, Dec. 2011. ISSN 1752-0509. doi: 10.1186/1752-0509-5-198. URL <http://www.biomedcentral.com/1752-0509/5/198/abstract>.

Reproducibility report for: A Quantitative Model of Human Jejunal Smooth Muscle Cell Electrophysiology.

Submitted to: *Physiome*

Manuscript number/identifier: S000009

Curation outcome summary: Successfully reproduced all the figures presented in this manuscript.

Box 1: Criteria for repeatability and reproducibility

■ **Model source code provided:**

- Source code: a standard procedural language is used (e.g. MATLAB, Python, C)
 - There are details/documentation on how the source code was compiled
 - There are details on how to run the code in the provided documentation
 - The initial conditions are provided for each of the simulations
 - Details for creating reported graphical results from the simulation results

■ Source code: a declarative language is used (e.g. SBML, CellML, NeuroML)

- The algorithms used are defined or cited in previous articles
- The algorithm parameters are defined
- Post-processing of the results are described in sufficient detail

Executable model provided:

- The model is executable without source (e.g. desktop application, compiled code, online service)
 - There are sufficient details to repeat the required simulation experiments

■ **The model is described mathematically in the article(s):**

- Equations representing the biological system
- There are tables or lists of parameter values
- There are tables or lists of initial conditions
- Machine-readable tables of parameter values
- Machine-readable tables of initial conditions

■ **The simulation experiments using the model are described mathematically in the article:**

- Integration algorithms used are defined
- Stochastic algorithms used are defined
- Random number generator algorithms used are defined
- Parameter fitting algorithms are defined
- The paper indicates how the algorithms yield the desired output

Box 2: Criteria for accessibility

- Model/source code is available at a public repository or researcher's web site
 - Prohibitive license provided
 - Permissive license provided
 - Open-source license provided
- All initial conditions and parameters are provided
- All simulation experiments are fully defined (events listed, collection times and measurements specified, algorithms provided, simulator specified, etc.)

Box 3: Rules for Credible practice of Modeling and Simulation^a

^aModel credibility is assessed using the Interagency Modeling and Analysis Group conformance rubric:
<https://www.imagwiki.nibib.nih.gov/content/10-simple-rules-conformance-rubric>

- Define context clearly: Extensive
- Use appropriate data: Extensive
- Evaluate within context: Extensive
- List limitations explicitly: Insufficient
- Use version control: Extensive
- Document adequately: Extensive
- Conform to standards: Extensive

Box 4: Evaluation

- Model and its simulations could be repeated using provided declarative or procedural code
- Model and its simulations could be reproduced

Summary comments: Model and source code are available in the associated OMEX archive. This was used in our attempt to reproduce the results presented in the paper. We successfully ran the python scripts provided to reproduce Figure 1 - Figure 8 as presented in this manuscript.



Anand K. Rampadarath¹, PhD
Curator
Center for Reproducible Biomedical Modeling
Auckland Bioengineering Institute,
University of Auckland



Herbert M. Sauro, Professor
Director
Center for Reproducible Biomedical Modeling
University of Washington,
Seattle, WA

¹Email: a.rampadarath@auckland.ac.nz